19

Formation of silver nanoparticles oligomers obtained via laser ablation in a liquid by sequential centrifugation and ultrasonication: tunable long-wavelength shift of plasmon resonance for biomedical applications

© D.R. Dadadzhanov[1], A.V. Palekhova[1], G. Alexan[1], M.A. Baranov[1], N.A. Maslova[2]

[1] International Research and Education Center for Physics of Nanostructures, ITMO University, 197101 St. Petersburg, Russia
[2] Research Park, Saint Petersburg State University, 199034 St. Petersburg, Russia

e-mail: daler.dadadzhanov@gmail.com

Received May 12, 2023
Revised May 12, 2023
Accepted May 26, 2023

A relatively simple physical method has been proposed for fabrication of stable oligomers of silver nanoparticles, preliminarily obtained by pulsed laser ablation of a metal target in a liquid. Oligomers of silver nanoparticles are formed in an aqueous solution after prolonged centrifugation at 18000 g and subsequent ultrasonication of the initial colloidal solution of spherical nanoparticles obtained by laser ablation. The plasmon resonance in oligomers is shifted relative to the plasmon resonance in spherical nanoparticles to the long wavelength region by 140 nm.

Keywords: plasmon resonance, silver nanoparticles, laser ablation, extinction.

DOI: 10.61011/EOS.2023.07.57142.5120-23

Introduction

Metal nanoparticles made of silver and gold are widely used in such areas as targeted drug delivery [1], photothermal [2] and photodynamic [3] cancer therapy, optical coherence tomography, immunoassay [4,5] and biosensing [6–8]. Considerable attention is paid to nanoparticles in the study of physiological structures and cellular functions *in vitro* and *in vivo*. Interest in the use of metal nanoparticles is explained by their unique optical and catalytic properties, which depend on the size and shape of nanoparticles [9]. The optical properties of metal nanoparticles are determined by the excitation of localized surface plasmonic resonance, which arises as a result of the interaction of electromagnetic radiation and collective oscillations of conduction electrons in the nanoparticle. Studying the influence of the physicochemical properties of nanoparticles, including their shape, size, surface charge, surface chemistry and cytotoxicity, on the efficiency of endocytosis — cellular attenuation and cell survival, is critical for the diagnosis and treatment of various disorders in living systems [10–13].

The rapid development of methods for the chemical synthesis of metal nanoparticles has opened up the possibility of obtaining nanoparticles in the form of nanospheres, nanorods, nanocubes, nanostars or nanolattices. On the other hand, various nanostructures with completely controlled spatial parameters can be formed using electron beam and „nanosphere“ lithographies. Pulsed laser ablation (LA) in liquids allows to obtain nanoparticles from a bulk target or thin-film materials [14–16]. This method is characterized by a high yield of nanoparticles, as well as simplicity, which eliminates the multi-step procedures required for chemical synthesis methods. From the point of view of biomedical applications, LA is distinguished by a high degree of purity of nanoparticles, which excludes the cytotoxic effect of chemical precursors. Many studies have already been carried out on the process of formation of metal nanoparticles during LA, starting with the influence of the solvent during synthesis [17,18] and the characteristics of the laser pulse, namely repetition rate and duration [19,20], as well as wavelength laser radiation [21–25] and ending with the influence of other experimental conditions, such as impurities and stabilizers [26–32]. It is reported that at low laser fluence, quasi-spherical nanoparticles with a narrow size distribution are typically formed, the stability of which is achieved due to electrostatic repulsion and the Van der Waals force, since both interactions contribute to the total free energy of the system [33,34]. It is also known that repeated exposure to laser radiation on formed nanoparticles leads to their fragmentation, making the nanoparticles even more spherical [21].

It is worth noting that the generation of anisotropic particles is not typical for LA. The spherical shape of nanoparticles is explained by the surface tension of the melt, because it is the sphere that has the minimum surface energy compared to other forms of nanoparticles. Nevertheless, there are several papers [35–37] devoted to the formation of anisotropic gold nanoparticles both in an aqueous medium and with the addition of $CaCl_2$ or $MgSO_4$ impurities, as well as in a magnetic field. However, the plasmon resonance in the mentioned papers is significantly broadened, which limits the use of nanoparticles obtained by such methods in biosensors. There have been attempts to fabricate silver nanoribbons using picosecond ablation

and further utilizing as SERS substrates for detecting explosives. Although NPs look like nanoribbons in shape, they lack characteristic spectral features in the long-wavelength spectral range [38]. The above review of approaches for preparing nanoparticles of complex shape confirms the need to develop simple and affordable methods for the synthesis of anisotropic metal nanoparticles with controlled optical properties and free from undesirable impurities.

In this paper, we propose a new method for the formation of anisotropic silver nanoparticles (NPs). While many studies on laser ablation are aimed at preventing the aggregation of NP, the idea of this paper is the opposite, namely, to establish conditions for the formation of aggregates that allow to obtain in a simple way anisotropic nanostructures — NP oligomers with plasmonic resonances in the long-wavelength spectral range. The main stages of the proposed method are to obtain a colloidal solution of nanoparticles of a predominantly spherical shape by laser ablation of a metal target in a liquid, centrifugation of the resulting colloidal solution, leading to the precipitation of large aggregates, and, finally, the formation of a colloidal solution of oligomers as a result of ultrasonication. The formation of oligomers of silver NPs is confirmed by analysis of images obtained on a scanning electron microscope, as well as by absorption spectroscopy methods. The influence of the parameters of laser irradiation, centrifugation and ultrasonication on the shape of nanoparticles was studied. A possible mechanism for the formation of NP oligomers obtained as a result of laser ablation is discussed.

Experimental part

Colloidal silver NPs were prepared using a pulsed laser ablation method in a liquid. A solid-state Nd:YAG laser (SOLAR Laser Systems, Belarus) with an intracavity second-harmonic generator was used as a radiation source, emitting pulses in Q-switch mode with a duration of 10 ns at a wavelength of 532 nm. Pulse repetition rate was 5 and 10 Hz. The energy of laser pulses was attenuated using NS-1 optical neutral filters. The laser beam diameter was 8 mm. The laser fluence varied in the range from 30 to 120 mJ/cm^2. Before the experiments, the silver target (99.99%) was cleaned by ultrasound in water, washed with ethanol and deionized water. Next, for the synthesis of NPs, the silver target was placed in a glass test tube with deionized water (18.2 MΩ· cm) with a volume of 5 ml. The height of the liquid level above the target was 20 mm. To focus laser radiation on a silver target, a collecting lens with a focal length $f = 90$ mm was used. After laser ablation of the target, the concentration of the obtained NPs was determined by measuring the mass of the material removed from the surface. The formation of oligomers of silver NP occurred during centrifugation of the resulting colloidal solutions of NP at an acceleration of 18000 g for a time t_{CF} in the range from 30 to 120 min. After sedimentation, the test tubes with NP were immersed in an ultrasonic bath. The t_{US} ultrasonication time varied in the range from 5 s to 5 min. The extinction spectra of colloidal nanoparticles were recorded using an SF-56 spectrophotometer (OKB Spektr, Russia).

Results and discussion

Figure 1, *a* shows the optical density spectra (extinction) of colloidal solutions of silver NPs obtained by laser ablation, depending on the duration of irradiation (t_{LA}), and in Fig. 1, *b* shows the effect of further centrifugation at 18000 g and ultrasonication. Formation of colloidal silver nanoparticles was carried out at an laser fluence of 30 mJ/cm^2 and a exposure duration of 60 and 90 min (Fig. 1, *a*). The selected irradiation time provide a sufficiently high concentration of the NPs in solution to prepare a large number of aggregates.

The wide bandwidth of the extinction spectrum indicates its heterogeneous broadening associated with the size distribution of Ag NPs (Fig. 1, *a*). Increasing the duration of irradiation leads to an increase in the concentration of Ag NPs in the solution, but the spectral position of the maximum of the plasmon resonance of Ag NPs at a wavelength of 404 nm remains unchanged, which is in good agreement with the literature data [39]. The extinction spectrum (Fig. 1, *a*) also has a long-wavelength shoulder in the area of 530 nm.

Colloidal solutions of Ag NPs as a result of LA (Fig. 1, *a*, red curve) were firstly centrifugated, and then a Eppendorf tube with Ag NPs was immersed in an ultrasonic bath and subjected to ultrasonication during $t_{US} = 5$ s. As a result, the absorbance in the range of the plasmonic band decreased, and its maximum shifted by 6 nm to the longer wavelength side (Fig. 1, *b*, black curve). On the other hand, an increase in absorbance in the range of 530 nm indicates an increase in the number of aggregated forms of Ag NPs as a result of a violation of solution stability, since, in contrast to chemical synthesis methods [40–42], the LA method leads to the production of solutions of NPs, which do not contain stabilizing agents. Increasing the duration of centrifugal deposition to $t_{CF} = 120$ min leads to a further decrease in the absorbance in the area of the plasmonic band and an increase in the relative contribution of aggregated forms of Ag NP. The long-wavelength shoulder, which becomes noticeable with increasing t_{CF}, probably reflects the interaction between individual NPs within aggregates [43,44].

The extinction spectra in Fig. 2 show the effects of centrifugation and ultrasonication time on the formation of aggregated forms for two colloidal solutions of NPs obtained at laser ablation duration $t_{LA} = 60$ min and two different laser fluence $E = 60$ mJ/cm^2 (fig. 2, *a*) and $E = 120$ mJ/cm^2 (fig. 2, *b*), respectively.

Comparing the black curves of Fig. 2, *a* and 2, *b*, it can be seen that with an increase laser fluence of pulses with their total number unchanged, the absorbance in the plasmonic

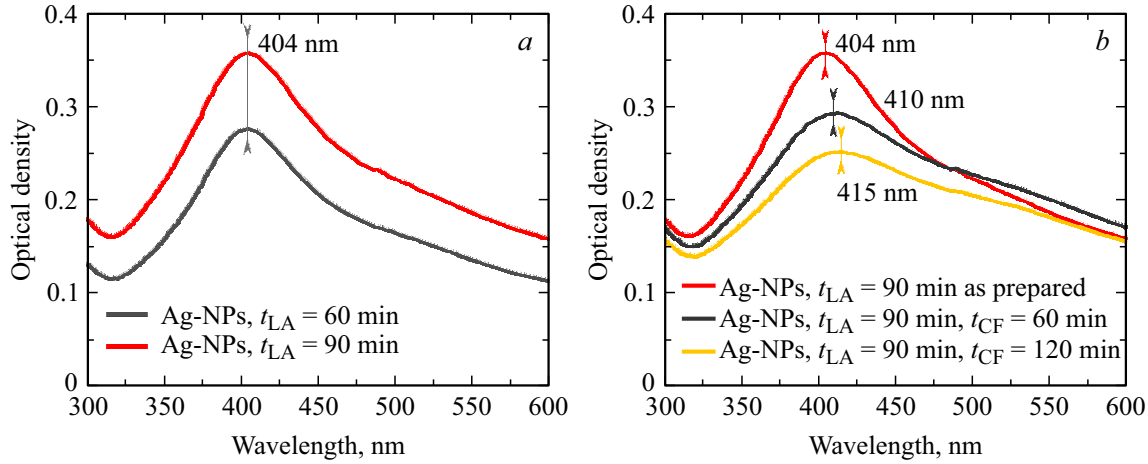

Figure 1. Extinction spectra of Ag NP in deionized water during LA with energy density $E = 30\,\text{mJ/cm}^2$. (*a*) Colloidal solution of Ag NP obtained as a result of laser ablation (pulse repetition rate 10 Hz) for $t_{LA} = 60$ min (black curve) and $t_{LA} = 90$ min (red curve). (*b*) Colloidal solution of Ag NPs during LA for $t_{LA} = 90$ min before (red curve) and after centrifugation (centrifugal acceleration 18000 g) for $t_{CF} = 60$ and 120 min (black and yellow curves, respectively) and subsequent ultrasonication during $t_{US} = 5$ s.

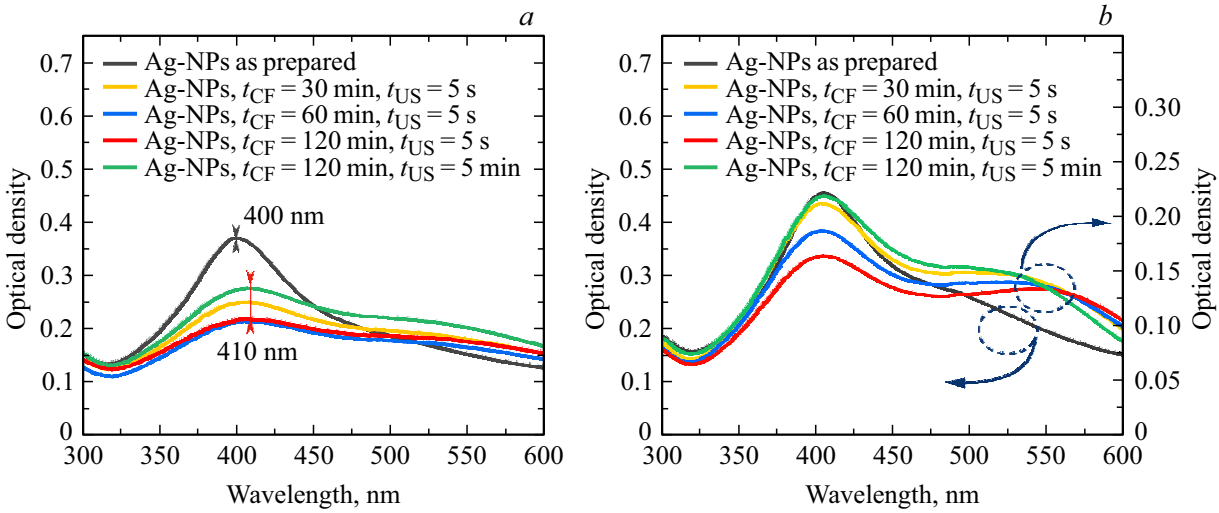

Figure 2. Extinction spectra of colloidal solutions of Ag NPs obtained by the LA method in deionized water at laser fluence $E = 60\,\text{mJ/cm}^2$ (*a*) and $E = 120\,\text{mJ/cm}^2$ (*b*). Pulse repetition rate 10 Hz, irradiation time $t_{LA} = 60$ min. The absorbance of colloidal solutions obtained directly as a result of laser ablation is shown by black curves, and after centrifugation and ultrasonication by colored curves. The durations of centrifugation and ultrasonication are given in the figure field.

resonance area increases, and the plasmonic absorption band itself becomes less symmetrical. The influence of the duration of centrifugation (t_{CF} from 30 to 120 min) and the duration of exposure to ultrasound (t_{US}) n the extinction spectra of colloidal NPS can be seen in Fig. 2 using the example of two samples obtained at different laser fluence $E = 60\,\text{mJ/cm}^2$ (fig. 2, *a*) and $E = 120\,\text{mJ/cm}^2$ (fig. 2, *b*). The main changes are observed in the absorption band in the range of $\lambda = 550$ nm, most significantly at the maximum laser fluence of pulses $E = 120\,\text{mJ/cm}^2$ (Fig. 2, *b*) and the maximum duration of exposure to ultrasound $t_{US} = 5$ min. Under these conditions, a new absorption band is formed with a maximum at the wavelength of $\lambda = 550$ nm. Increasing the duration of exposure to ultrasound in all cases leads to an increase in the optical density of the colloidal NPs due to additional defragmentation of precipitated NPs. At the laser fluence $E = 30\,\text{mJ/cm}^2$, changes in the optical characteristics after centrifugation and ultrasonication were insignificant (data are not shown).

Figure 3 shows the normalized extinction spectra of colloidal solutions of Ag NPs exposed to laser radiation with a lower pulse repetition rate (5 Hz). Reducing the laser pulse repetition rate by a factor of two led to a noticeable narrowing of the plasmonic resonance band (Fig. 3, black curve), despite the close values of the laser fluence of pulses (Fig. 1,*a*, black curve). On the other hand, doubling the irradiation time led to the appearance of an absorption band in the long-wave spectral range (Fig. 3, red curve).

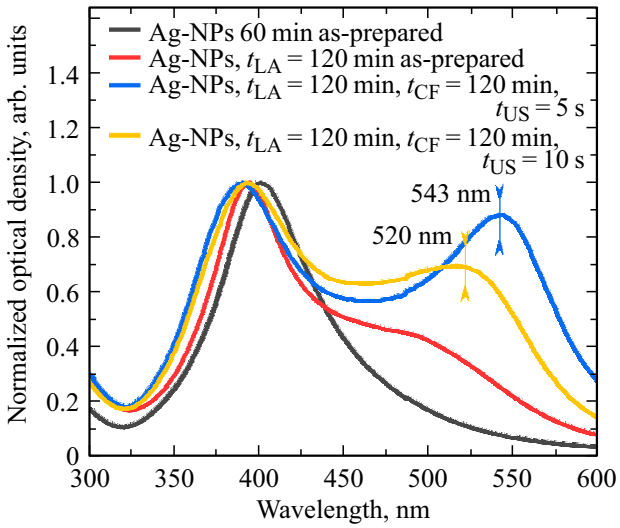

Figure 3. Extinction spectra of colloidal solutions of silver NPs after centrifugation and ultrasonication (colored curves), obtained as a result of laser ablation of a metal target in water with a pulse repetition rate of 5 Hz and laser radiation energy density $E = 40\,\text{mJ/cm}^2$ (black curve). All spectra are normalized to the maximum of the short-wavelength absorption band.

Centrifugation for $t_{CF} = 120$ min and ultrasonication for $t_{US} = 5$ s led to a significant increase in absorption in the long-wave band with a maximum at wavelength $\lambda = 543$ nm and a small (23 nm) short-wave shift of the short-wave band with a maximum in the range of 400 nm. Additional ultrasonication ($t_{US} = 10$ s) causes a weakening of the long-wavelength band and its short-wavelength shift, apparently associated with the collapse of NP aggregates.

Based on the obtained extinction spectra of colloidal solutions of Ag NPs, it is reasoble to associate the short-wave absorption band in the range of 400 nm with localized plasmon resonance in NPs close to a spherical shape, and the long-wave absorption band with a maximum in the range of 543 nm — with the formation of aggregates as a result of centrifugation. There are no conditions for the direct formation of nanorods that have similar absorption spectra [40,45,46]. At the same time, the formation of dimers of individual spherical NPs under the conditions of the described experiments is very likely and leads to observable changes in the extinction spectra [47].

To determine the morphology of silver NPs, their images were obtained using a scanning electron microscope (SEM) (Fig. 4). Colloidal silver NPs were preliminarily deposited onto a silicon substrate before measurements. Two SEM images of NPs before centrifugation are shown in panels 1 and 2 of Fig. 4. The corresponding extinction spectrum of NPs for an LA duration $t_{LA} = 120$ min is shown in Fig. 3 (*red curve*). It follows from the SEM-images that long-term laser ablation leads to the formation of both individual quasi-spherical NPs (panel 1) with sizes ranging from 5 to 200 nm, and aggregated NPs (panel 2) in the form of branching structures, the total size of which exceeds the wavelength incident radiation. The presence of individual NPs with inhomogeneous size and complex structures leads to a broadening of the plasmonic resonance in the extinction spectrum before centrifugation. At the same time, the appearance of a strongly pronounced shoulder in Fig. 3 (red curve) is explained by morphological changes in NPs as a result of self-assembly of quasi-spherical NPs of different sizes into complex structures.

After centrifugation and ultrasonication doubling the irradiation time led to the appearance of an absorption band in the long-wave spectral area (Fig. 3, red curve). Centrifugation for $t_{CF} = 120$ min and ultrasonication for $t_{US} = 5$ s led to a significant increase in absorption in the long-wave band with a maximum at wavelength $\lambda = 543$ nm and a small (23 nm) short-wave shift of the short-wave band with a maximum in the range of 400 nm. Additional ultrasonication ($t_{US} = 10$ s) causes a weakening of the long-wave band and its short-wave shift, apparently associated with the repetition of this sample in the SEM images shown in Fig. 4 (panels 3 and 4), the formation of oligomer-like NPs is observed [48]. This fact correlates well with the appearance of a long-wavelength band with a maximum in the approximaty of 543 nm in the extinction spectrum (Fig. 3, blue curve).

Figure 4 also shows SEM images of silver NPs (panels 5 and 6) before and after centrifugation and ultrasonication (panels 7 and 8). The extinction spectrum in Fig. 2, *b* for silver NPs in panels 5 and 6 is presented as a black curve, and in panels 7 and 8 it is displayed as a red curve. It is important to note that the heterogeneous of the substrate in the form of a labyrinthine structure on panels 5 and 6 should not be attributed to silver NP. The areas directly related to the NPs themselves are highlighted in blue. It follows from the images that immediately after LA, oligomers are formed from relatively identical NPs in size and shape [48], and with subsequent centrifugation and ultrasonication of the NPs (panels 7 and 8), their density increases.

Thus, it has been established that the formation of oligomer-like NPs occurs under conditions of high NP concentration (approximately 1 mM), which is achieved as a result of long-term laser ablation of a silver target. After centrifugation and ultrasonication (Fig. 4, panels 4 and 8), oligomers are obtained more efficiently than immediately after LA. In addition, a more pronounced long-wavelength peak is observed only for oligomers from larger NPs obtained at a laser pulse repetition rate of 5 Hz. The significant difference in the results obtained at different laser pulse repetition rates can be explained by the fact that during laser ablation three competing processes are observed, namely: fragmentation of previously formed NP under the action of laser radiation, aggregation of NP with increasing concentration in water, and the formation of cavitation bubbles . The first process — NP fragmentation — arises as a result of repeated irradiation of formed NP in a liquid, since the laser radiation wavelength (532 nm) falls in the region of the long-wavelength shoulder in the absorption spectrum of silver NP [49]. On the other hand,

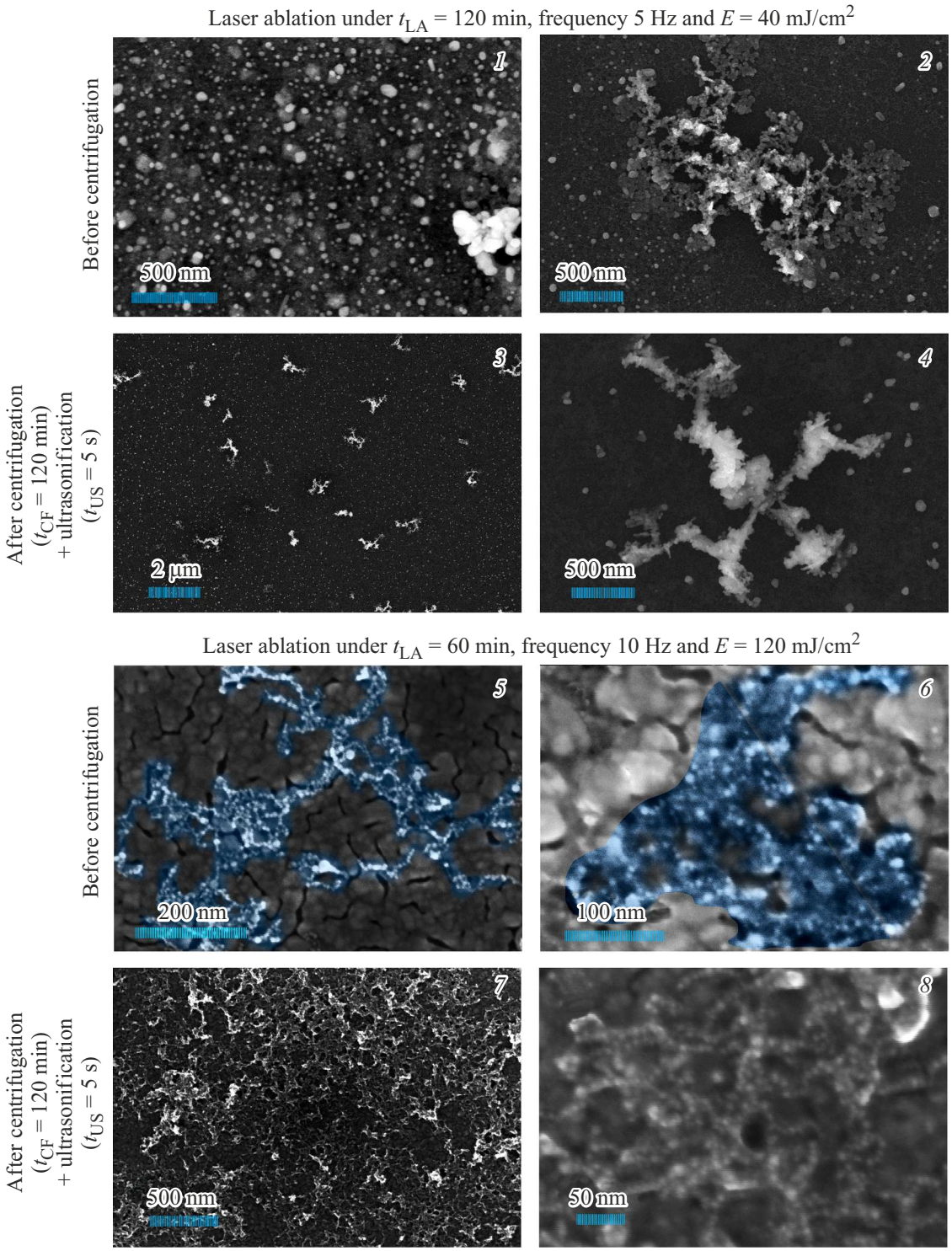

Figure 4. SEM images of silver NPs before and after centrifugation followed by ultrasonic treatment. The images in panels 1 and 2 correspond in Fig. 3 to the absorption spectrum of silver NPs before centrifugation (black curve), and 3 and 4 — after centrifugation (blue curve). The images in panels 5 and 6 refer to the extinction spectrum with the black curve in Fig. 2, *b*, and in 7 and 8 to the red curve. The bar shows the scale of the images.

despite the stabilizing role of electrostatic repulsion, as the concentration of NPs in the solution increases, the stability of the colloidal solution is partially disrupted, and oligomers are formed, as shown in Fig. 4 (panels 2 and 6). It is also known that with an increase in the pulse repetition rate due to an increase in the temperature of the liquid, cavitation microbubbles are formed, which defocus and screen the laser radiation. Therefore, at a laser pulse repetition rate of

10 Hz, the screening of incident radiation was stronger due to the relatively larger number of microbubbles than at 5 Hz. Consequently, with an increase in the pulse repetition rate, the probability of fragmentation of large NP resonant with incident radiation during LA increases. This is confirmed by the morphology of the NPs in the SEM images (Fig. 4, panel 5 and 6) before centrifugation.

Conclusion

A new method has been developed for the formation of oligomers of nanoparticles in an aqueous solution, which includes the following operations: formation a colloidal solution of metal nanoparticles, predominantly spherical in shape, by ablation of a metal target with pulsed laser radiation, sedimentation of the colloidal solution as a result of centrifugation, and transfer of the oligomers of metal nanoparticles formed in the sediment into the colloidal solution by ultrasonication. Conformation of individual nanoparticles and their oligomers is confirmed by consistent data from absorption spectroscopy and electron microscopy. It was found that at short irradiation and centrifugation times, the probability of the formation of oligomeric nanoparticles is low. Colloidal solutions obtained under these conditions are stable for months. Thus, due to the ability to tune plasmon resonance to the long-wavelength spectral range without using conventional chemical synthesis method, surfactant-free silver nanoparticle oligomers can find wide application in biomedical imaging, targeted drug delivery, and photothermal therapy.

Acknowledgments

SEM-studies were carried out on the equipment of the Interdisciplinary Resource Center of „Nanotechnology “ of St. Petersburg State University Science Park.

Funding

This work was supported by the Russian Science Foundation (Project 22-72-10057)

Conflict of interest

The authors declare that they have no conflict of interest.

References

[1] V. Chandrakala, V. Aruna, G. Angajala. Emergent Materials, **5** (6), 1593–1615 (2022). DOI: 10.1007/S42247-021-00335-X
[2] M. Kim, J.H. Lee, J.M. Nam. Advanced Science, **6** (17), 1900471 (2019). DOI: 10.1002/ADVS.201900471
[3] T. Liu, Y. Song, Z. Huang, X. Pu, Y. Wang, G. Yin, L. Gou, J. Weng, X. Meng. Colloids Surf B Biointerfaces, **207**, 112023 (2021). DOI: 10.1016/J.COLSURFB.2021.112023
[4] Y. Gao, Y. Zhou, R. Chandrawati. ACS Appl Nano Mater., **3** (1), 1–21 (2020). DOI: 10.1021/ACSANM.9B02003
[5] H. Yang, W. Xu, Y. Zhou. Microchimica Acta, **186** (12), 1–22 (2019). DOI: 10.1007/S00604-019-3904-9
[6] H. Malekzad, P. Sahandi Zangabad, H. Mirshekari, M. Karimi, M.R. Hamblin. Nanotechnol Rev., **6** (3), 301–329 (2017). DOI: 10.1515/NTREV-2016-0014
[7] D.R. Dadadzhanov, I.A. Gladskikh, M.A. Baranov, T.A. Vartanyan, A. Karabchevsky. Sens. Actuators B Chem., **333**, 129453 (2021). DOI: 10.1016/J.SNB.2021.129453
[8] G.A. Sotiriou. Wiley Interdiscip Rev Nanomed Nanobiotechnol., **5** (1), 19–30 (2013). DOI: 10.1002/WNAN.1190
[9] K.L. Kelly, E. Coronado, L.L. Zhao, G.C. Schatz. J. Phys. Chem. B., **107** (3), 668–677 (2003). DOI: 10.1021/JP026731Y
[10] L. Ding, C. Yao, X. Yin, C. Li, Y. Huang, M. Wu, B. Wang, X. Guo, Y. Wang, M. Wu. Small, **14** (42), 1801451 (2018). DOI: 10.1002/SMLL.201801451
[11] K. Kettler, K. Veltman, D. van de Meent, A. van Wezel, A.J. Hendriks. Environ. Toxicol. Chem., **33** (3), 481–492 (2014). DOI: 10.1002/ETC.2470
[12] P. Gurnani, C. Sanchez-Cano, H. Xandri-Monje, J. Zhang, S.H. Ellacott, E.D.H. Mansfield, M. Hartlieb, R. Dallmann, S. Perrier, Small, **18** (38), 2203070 (2022). DOI: 10.1002/SMLL.202203070
[13] N.N. Zhang, H.R. Sun, S. Liu, Y.C. Xing, J. Lu, F. Peng, C.L. Han, Z. Wei, B. Yang, K. Liu. CCS Chemistry, **4** (2), 660–670 (2022). DOI: 10.31635/ccschem.021.202000637
[14] A. Takami, H. Kurita, S. Koda. J. Phys. Chem. B, **103** (8), 1226–1232 (1999). DOI: 10.1021/JP983503O
[15] V. Amendola, M. Meneghetti. Physical Chemistry Chemical Physics, **15** (9), 3027–3046 (2013). DOI: 10.1039/C2CP42895D
[16] F. Mafun., J.Y. Kohno, Y. Takeda, T. Kondow, H. Sawabe. J. Phys. Chem. B, 104 (39), 9111–9117 (2000). DOI: 10.1021/JP001336Y
[17] V. Amendola, S. Polizzi, M. Meneghetti. Langmuir, **23** (12), 6766–6770 (2007). DOI: 10.1021/LA0637061
[18] S.M. Arakelyan, V.P. Veiko, S.V. Kutrovskaya, A.O. Kucherik, A.V. Osipov, T.A. Vartanyan, T.E. Itina. J. Nanoparticle Research, **18** (6), 1–12 (2016). DOI: 10.1007/S11051-016-3468-0
[19] R. Zamiri, A. Zakaria, H.A. Ahangar, M. Darroudi, G. Zamiri, Z. Rizwan, G.P.C. Drummen. Int J Nanomedicine, **8** (1), 233–244 (2013). DOI: 10.2147/IJN.S36036
[20] A. Hahn, S. Barcikowski, B.N. Chichkov. Journal of Laser Micro Nanoengineering, **3** (2), 73–77 (2009). DOI: 10.2961/JLMN.2008.02.0003
[21] V. Piotto, L. Litti, M. Meneghetti. Journal of Physical Chemistry C, **124** (8), 4820–4826 (2020). DOI: 10.1021/ACS.JPCC.9B10793
[22] J. Theerthagiri, K. Karuppasamy, S.J. Lee, R. Shwetharani, H.S. Kim, S.K.K. Pasha, M. Ashokkumar, M.Y. Choi. Light: Science & Applications, **11** (250), 1–47 (2022). DOI: 10.1038/s41377-022-00904-7
[23] M. Ratti, J.J. Naddeo, J.C. Griepenburg, S.M. O'Malley, D.M. Bubb, E.A. Klein. J. Vis. Exp., (124), 55416 (2017). DOI: 10.3791/55416
[24] D. Dıaz, A. Molina, D. Hahn. Spectrochim Acta Part B At Spectrosc., **145**, 86–95 (2018). DOI: 10.1016/J.SAB.2018.04.007

[25] T. Mohamed, M.H. El-Motlak, S. Mamdouh, M. Ashour, H. Ahmed, H. Qayyum, A. Mahmoud. Materials, **15** (20), 7348 (2022). DOI: 10.3390/MA15207348
[26] V. Scardaci, M. Condorelli, M. Barcellona, L. Salemi, M. Pulvirenti, M.E. Fragalá, G. Applied Sciences, **11** (19), 8949 (2021). DOI: 10.3390/APP11198949/S1
[27] F.Y. Alzoubi, J.Y. Al-zou'by, S.K. Theban, M.K. Alqadi, H.M. Al-khateeb, E.S. AlSharo, Nanotechnology for Environmental Engineering, **6** (3), 1–7 (2021). DOI: 10.1007/S41204-021-00165-6
[28] T. Tsuji, M. Tsuji, S. Hashimoto. J. Photochem. Photobiol. A Chem., **221** (2), 224–231 (2011). DOI: 10.1016/J.JPHOTOCHEM.2011.02.020
[29] V. Amendola, M. Meneghetti. Physical Chemistry Chemical Physics, **11** (2), 3805–3821 (2009). DOI: 10.1039/B900654K
[30] G. Wang, C. Yan, S. Gao, Y. Liu. Materials Science and Engineering: C, **103**, 109856 (2019). DOI: 10.1016/J.MSEC.2019.109856
[31] K. Bolaños, M.J. Kogan, E. Araya. Int. J. Nanomedicine, **14**, 6387–6406 (2019). DOI: 10.2147/IJN.S210992
[32] J.P. Sylvestre, S. Poulin, A.V. Kabashin, E. Sacher, M. Meunier, J.H.T. Luong. Journal of Physical Chemistry B, **108** (43), 16864.–6869 (2004). DOI: 10.1021/JP047134
[33] K.K. Kim, H.J. Kwon, S.K. Shin, J.K. Song, S.M. Park. Chem Phys Lett., **588**, 167–173 (2013). DOI: 10.1016/J.CPLETT.2013.10.011
[34] E. Fazio, B. Gökce, A. De Giacomo, M. Meneghetti, G. Compagnini, M. Tommasini, F. Waag, A. Lucotti, C.G. Zanchi, P.M. Ossi, M. Dell'aglio, L. D'urso, M. Condorelli, V. Scardaci, F. Biscaglia, L. Litti, M. Gobbo, G. Gallo, M. Santoro, S. Trusso, F. Neri. Nanomaterials, **10** (11), 2317 (2020). DOI: 10.3390/NANO10112317
[35] M.I. Zhilnikova, E.V. Barmina, G.A. Shafeev, S.M. Pridvorova, O.V. Uvarov. Gold Bull., **53** (3), 129–134. DOI: 10.1007/S13404-020-00281-2
[36] M.I. Zhil'nikova, E.V. Barmina, G.A. Shafeev. Physics of Wave Phenomena, **26** (2), 85–92 (2018). DOI: 10.3103/S1541308X18020024
[37] A.V. Simakin, I.V. Baimler, V.V. Smirnova, O.V. Uvarov, V.A. Kozlov, S.V. Gudkov. Physics of Wave Phenomena, **29** (2), 102–107 (2021). DOI: 10.3103/S1541308X21020126
[38] H. Marrapu, R. Avasarala, V.R. Soma, S.K. Balivada, G.K. Podagatlapalli. RSC Adv., **10** (67), 41217–41228 (2020). DOI: 10.1039/D0RA05942K
[39] H. Qayyum, W. Ahmed, S. Hussain, G.A. Khan, Z.U. Rehman, S. Ullah, T.U. Rahman, A.H. Dogar. Opt Laser Technol., **129**, 106313 (2020). DOI: 10.1016/J.OPTLASTEC.2020.106313
[40] A. Heuer-Jungemann, N. Feliu, I. Bakaimi, M. Hamaly, A. Alkilany, I. Chakraborty, A. Masood, M.F. Casula, A. Kostopoulou, E. Oh, K. Susumu, M.H. Stewart, I.L. Medintz, E. Stratakis, W.J. Parak, A.G. Kanaras. Chem Rev., **119** (8), 4819–4880 (2019). DOI: 10.1021/ACS.CHEMREV.8B00733
[41] Z.C. Xu, C.M. Shen, C.W. Xiao, T.Z. Yang, H.R. Zhang, J.Q. Li, H.L. Li, H.J. Gao. Nanotechnology, **18** (11), 115608 (2007). DOI: 10.1088/0957-4484/18/11/115608
[42] D. Rioux, M. Meunier. J. Phys. Chem. C, **119** (23), 13160–13168 (2015). DOI: 10.1021/ACS.JPCC.5B02728
[43] F. Dong, E. Valsami-Jones, J.U. Kreft. J. Nanoparticle Research, **18** (9), 1–12 (2016). DOI: 10.1007/S11051-016-3565-0
[44] M.C. Sportelli, M. Clemente, M. Izzi, A. Volpe, A. Ancona, R.A. Picca, G. Palazzo, N. Cioffi. Colloids Surf. A Physicochem. Eng. Asp., **559**, 148–158 (2018). DOI: 10.1016/J.COLSURFA.2018.09.046
[45] A. Rao, H. Cölfen. Comprehensive Supramolecular Chemistry II, (Elsevier, Walthm, MA, USA, 2017), p. 129–156. DOI: 10.1016/B978-0-12-409547-2.12638-1
[46] B. Khodashenas, H.R. Ghorbani. Arabian J. Chemistry, **12** (9), 1823–1838 (2019). DOI: 10.1016/J.ARABJC.2014.12.014
[47] W. Li, P.H.C. Camargo, X. Lu, Y. Xia. Nano Lett., **9** (1), 485–490 (2009). DOI: 10.1021/NL803621X
[48] H.A. Alluhaybi, S.K. Ghoshal, W.N.W. Shamsuri, B.O. Alsobhi, A.A. Salim, G. Krishnan. Nano-Structures & Nano-Objects, **19**, 100355 (2019). DOI: 10.1016/J.NANOSO.2019.100355
[49] A.R. Ziefuß, S. Reichenberger, C. Rehbock, I. Chakraborty, M. Gharib, W.J. Parak, S. Barcikowski. J. Phys. Chem. C, **122** (38), 22125–22136 (2018). DOI: 10.1021/ACS.JPCC.8B04374
[50] M.A. Valverde-Alva, T. Garcıa-Fernández, E. Esparza-Alegrıa, M. Villagrán-Muniz, C. Sánchez-Aké, R. Castañeda-Guzmán, M.B. De La Mora, C.E. Márquez-Herrera, J.L. Sánchez Llamazares. Laser Phys. Lett., **13** (10), 106002 (2016). DOI: 10.1088/1612-2011/13/10/106002
[51] A. Menéndez-Manjón, B.N. Chichkov, S. Barcikowski. J. Phys. Chem. C, **114** (6), 2499–2504 (2010). DOI: 10.1021/JP909897V

Translated by Ego Translating